DOI: 10.1002/ejic.200800236

Synthesis of Manganese Oxide Hollow Urchins with a Reactive Template of Carbon Spheres

Nan Wang,[a] Yu Gao,[a] Jian Gong,*[a] Xinyan Ma,[a] Xiaoli Zhang,[a] Yihang Guo,[a] and Lunyu Qu[a]

Keywords: Carbon spheres / Template synthesis / Manganese / Hollow urchins

In this paper, a novel route to synthesize manganese oxide (MnO_2) hollow urchins by a reactive template of carbon spheres is described. The formation process of the MnO_2 hollow urchins and the mechanism for the removal of the carbon spheres are suggested. The results of scanning electron microscopy and transmission electron microscopy indicate that MnO_2 shows a hollow-urchin structure with an average diameter of 1.5 μm and with cavities that are about 250–500 nm in diameter. The X-ray diffraction pattern indicates that the as-prepared hollow urchins are γ-MnO_2. It has a high Brunauer–Emmett–Teller surface area of 110 $m^2 g^{-1}$ and a mesoporous structure. In addition, the magnetic properties of the γ-MnO_2 hollow urchins are investigated. This method opens a way to obtain different morphologies of metal oxides by changing the morphologies of the reactive carbon template.

Introduction

The ability to synthesize hollow structures possessing tailored properties, such as higher specific surface area, porosity, lower density, or good permeation, is a topic of intense research activity in modern materials science. Particularly, considerable research interest has been focused on hollow metal oxides due to their potential applications as catalysts, adsorbents, sensors, photonic crystals, drug-delivery carriers, biomedical diagnosis agents, lightweight fillers, acoustic insulators, and chemical reactors.[1–6] Among the currently available fabrication methods, template-assisted synthesis, which uses different precursors as templates including polystyrene spheres,[7] spheres silica,[8] carbon,[9] liquid droplets,[10] micelles,[11] and microemulsion droplets,[12] is an efficient, controllable, and conventional route to prepare such materials. However, the removal of the template suffers from the drawbacks of high-temperature processing, special equipment and conditions, and tedious procedures such as calcination, wet chemical etching, and galvanic replacement, which results in disorder or destruction of the mesostructures and this can even affect the chemical structure of the as-prepared product. Therefore, research on controlling the morphology of order and pure hollow metal oxides by using only a convenient and green method has been needed in nanochemistry and nanotechnology.

Recently, a novel reactive template method was reported where polyaniline with octahedral and nanotubular morphology was obtained by using cuprous oxide and manganese oxide, respectively, as reactive templates.[13,14] In comparison to conventional template methods, this new method does not require additional dissolution nor a calcination process to remove the template cores, which reduces the number of processing steps.

Carbon, which possesses various morphologies, such as nanorods, spheres, and nanotubes, has been used as a very useful template to synthesize nanomaterials. For example, mesoporous spheres of metal oxides were synthesized by using mesoporous carbon atoms.[15] Hollow metal oxide nanofibers with a hierarchical architecture were synthesized by using activated carbon fibers as templates.[16] However, the post-treatment to remove the carbon template requires calcination of the carbon templates at high temperatures. To the best of our knowledge, no report has appeared concerning carbon as a reactive template to synthesize metal oxides with a hollow morphology. It is conceivable that if carbon with different morphologies could be used as a reactive template, metal oxides with corresponding morphologies would be prepared easily by this method, which is very significant for the rational control of the morphology and size of the materials and their chemical and physical properties.

As an important transition-metal oxide, manganese dioxide is one of the most attractive inorganic materials, because of its special physical and chemical properties and wide applications in catalysis, ion-exchanges processes, molecular adsorption, biosensing, magnetic applications, and especially its use as a cathode for batteries.[17–21] The properties

[a] Key laboratory of Polyoxometalate Science of Ministry of Education Faculty of Chemistry, Institute of Polyoxometalate Chemistry, Northeast Normal University,
Changchun 130024, China
Fax: +86-431-85099668
E-mail: gongj823@nenu.edu.cn

of MnO_2 are greatly affected by morphology, surface area, and the pore-size distribution. Thus, several techniques have been developed for the preparation of MnO_2 with controlled morphologies, including MnO_2 nanowires, nanorods, nanotubes, microspheres structures, etc.[22–26] Suib and coworkers reported a self-assembly synthesis of γ-MnO_2 mesoporous hollow nanospheres, which are composed of porous γ-MnO_2 hexagonal nanoflakes.[27] A solution-based catalytic route was promoted to synthesize various α-MnO_2 hierarchical structures and β-MnO_2 nanorods by Xie and coworkers.[28] However, the development of facile, mild, and effective methods for creating hollow MnO_2 nanomaterials with controllable sizes and morphologies is a new challenge faced by us.

In this paper, we describe a simple and rapid carbon-based reactive template method to synthesize bulk quantities of manganese oxide hollow spheres with urchin-like morphology. We find that carbon spheres can be oxidized in ammonium persulfate (APS) and $AgNO_3$ solution, which suggests that carbon spheres as a reactive template can be removed during the reaction at room temperature. Meanwhile, the formation mechanism, structural characteristics, and magnetic properties of the resulting manganese oxide hollow urchins are investigated. The Brunauer–Emmett–Teller (BET) specific surface area of the as-prepared γ-MnO_2 is 110 $m^2 g^{-1}$. This special high BET surface area of the hollow urchin structure provides the possibility of efficient transport of electrons in Li batteries. The most important aspect of our work, we think, is that this technology provides a general method to prepare structured oxides.

Results and Discussion

A typical scanning electron microscopy (SEM) image of carbon spheres produced by the hydrothermal treatment of a glucose/water solution without additives is shown in Figure 1. The diameters of the carbon spheres are about 200–500 nm. The surfaces of the synthesized carbon spheres are hydrophilic and functionalized with OH and C=O groups,[29] so the functional groups in the surface layer are able to bind metal cations through coordination or electrostatic interactions.

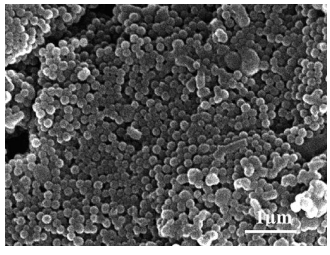

Figure 1. SEM image of carbon spheres obtained from the hydrothermal treatment of glucose.

Figure 2a shows the Fourier transform infrared (FTIR) spectrum of the carbon spheres. A broad absorption band at 3370 cm^{-1} is attributed to the hydroxy group. The bands at 1710 and 1620 cm^{-1}, which are attribute to the C=O and C=C vibrations, respectively, support the concept of aromatization of glucose during hydrothermal treatment. In the FTIR spectrum of the MnO_2 hollow urchins (Figure 2b), the above-mentioned bands have disappeared, indicating that the carbon spheres were removed during the reaction. The absorption bands at 470–710 cm^{-1} are assigned to the Mn–O stretching vibration of γ-MnO_2.[30,31]

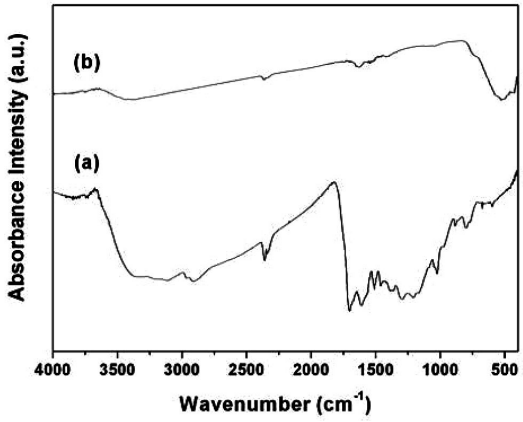

Figure 2. FTIR spectra of carbon spheres (a) and MnO_2 obtained from a typical reaction (b).

Figure 3 shows the X-ray diffraction (XRD) pattern of MnO_2 synthesized under the typical reaction conditions (APS 6 mol L^{-1} and $AgNO_3$ 0.0177 mol L^{-1}) at room temperature for 48 h. Notably, all the strong sharp diffraction peaks can be indexed as the pure orthorhombic phase of γ-MnO_2 with cell constants a = 6.36 Å, b = 10.15 Å, c = 4.09 Å, which are consistent with the values in the literature (JCPDS Card, No. 14–644).

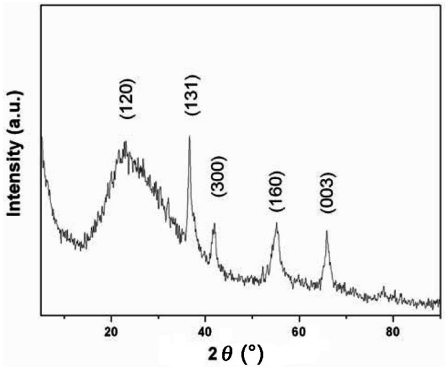

Figure 3. Typical XRD pattern of the as-prepared γ-MnO_2 hollow urchins.

Figure 4 shows the SEM and the transmission electron microscope (TEM) images of γ-MnO_2 obtained under the typical conditions (APS 6 mol L^{-1} and $AgNO_3$ 0.0177 mol L^{-1}) at room temperature for 48 h. Figure 4a shows that large-scale urchin-like microsphere structures with an average diameter of 1.5 μm were prepared. Moreover, these urchins exhibit interesting hollow structures. The

cavities with diameters of about 250–500 nm can be clearly seen from Figure 4b. To clarify the structures, a high-magnification image of an open urchin sphere is shown in Figure 4c, and it more clearly confirms the morphology of the cavity in γ-MnO_2. The shell of the structure consists of nanorods with diameters of about 25 nm and lengths in the range 100–500 nm (Figure 4d). Moreover, energy-dispersive spectroscopy (EDS) reveals that the hollow urchins are formed by Mn and O only with an atomic ratio of 1:2, as shown in Figure 4e. Elemental carbon cannot be detected in the resulting product, revealing that all of the carbon spheres were oxidized and no residue is present in the final products. These results indicate that hollow, urchin-like MnO_2 can be formed by using carbon spheres as reactive templates in the presence of APS and $AgNO_3$. Moreover, the carbon spheres template does not need to be removed after completion of the reaction, which simplifies the procedure. The morphology of the γ-MnO_2 hollow urchins is further investigated by TEM (Figure 4f). A visible dark–bright contrast between the boundary and the center of the spheres proves that these spheres are hollow spheres. The annular selected-area electron diffraction (SAED) pattern (Figure 4f, inset) indicates that the γ-MnO_2 hollow urchins are polycrystalline.

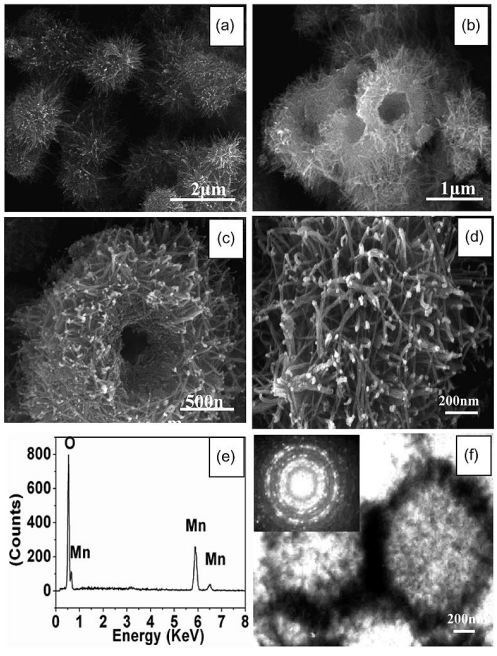

Figure 4. SEM and TEM images of MnO_2 hollow urchins synthesized by a reactive template route with a solution of APS (6 mol L^{-1}) and $AgNO_3$ (0.0177 mol L^{-1}). (a) Panoramic SEM image, (b) magnified SEM image, (c) typical open hollow urchins of the product, (d) high-magnification SEM image of the MnO_2 hollow urchins, (e) EDS of the hollow urchins, (f) TEM image of the MnO_2 hollow urchins. Inset shows the corresponding SAED pattern of the MnO_2 hollow urchins.

For a complete view of the mechanism of removal of the carbon spheres as a reactive template, oxidant-dependent evolutions of morphology were investigated by SEM. Figure 5 displays the SEM images of the product that was synthesized under the condition of 4 mol L^{-1} of APS and 0.0118 mol L^{-1} of $AgNO_3$. A low-magnification image (Figure 5a) clearly exhibits that the synthesized product possesses a sphere-like structure with a diameter of 1–2 μm. However, the surfaces of the spheres are significantly rough and possess a number of pores. From a high-magnification SEM image, we can clearly see the porous structure. Moreover, there are some small carbon spheres in the pores (as marked with white arrowheads in Figure 5b). Figure 5c displays a representative open sphere with a porous structure. The diameter of the pores is about 200 nm, which is consonant with the diameter of the carbon template as shown in Figure 1. In addition, small carbon spheres with smooth surfaces can be clearly seen in the pores. Obviously, the carbon template cannot be removed entirely owing to the lack of an oxidant. The EDS also shows that the porous spheres are mainly composed of Mn and O elements. However, a small amount of C is left (Figure 5d), which is consistent with the above result estimated from the SEM image.

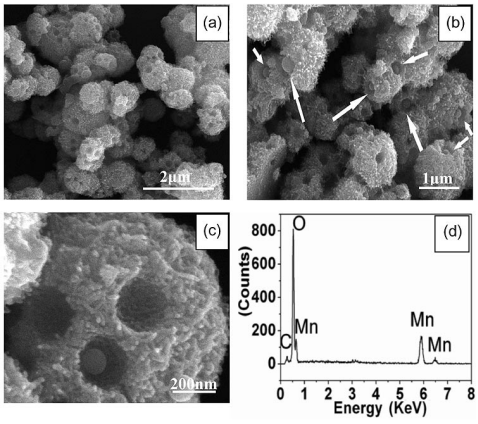

Figure 5. SEM images of porous spheres synthesized by a reactive template route with a solution of APS (4 mol L^{-1}) and $AgNO_3$ (0.0118 mol L^{-1}). (a) Low-magnification SEM image, (b) high-magnification SEM image of the product, (c) typical pores of the product, (d) EDS of the as-prepared porous spheres.

In order to verify the above results, we added carbon spheres into an APS solution in the presence of $AgNO_3$ and stirred the solution for 2 d. We found that the solution became transparent. However, if $AgNO_3$ is not introduced into the APS solution, under the same conditions the carbon spheres keep their morphology. This suggests that the carbon spheres can be removed in the mixed solution of APS and $AgNO_3$. As early as 1901, Marshall found that the oxidation of manganous ions could be carried out in the presence of silver ions as catalyst. Ordinarily, the oxidation of manganous ions by persulfate is very slow, but the silver-catalyzed reaction is remarkable. Investigation of the catalytic effect of silver ions on the reduction of peroxysulfates showed that the mechanism consists simply in the slow oxidation of the silver ions to the trivalent state and in subsequent rapid reaction between the oxidized silver and

manganous salt to form manganese oxide and univalent silver.[32–34]So, the possible mechanism for the removal of carbon spheres can be expressed by Equations (1), (2), and (3) [$E(Ag^{3+}/Ag^{+})$ = 1.89 V, $E(S_2O_8^{2-}/SO_4^{-})$ = 2.6 V, $E(SO_4^{-}/SO_4^{2-})$ = 2.43 V, $E(CO_2/C)$ = 0.207 V].[35–38]

$$S_2O_8^{2-} \rightarrow 2SO_4^{-} \quad (1)$$

$$2SO_4^{-} + Ag^{+} \rightarrow SO_4^{2-} + Ag^{3+} \quad (2)$$

$$2Ag^{3+} + C + 2H_2O \rightarrow 2Ag^{+} + CO_2 + 4H^{+} \quad (3)$$

From the above results, the formation process and mechanism can be suggested and concluded as follows: (1) Production of colloidal carbon spheres, which serve as a reactive templates, are first prepared from glucose starting materials under hydrothermal conditions. The surface of the carbon spheres is hydrophilic and functionalized with OH and C=O groups. (2) Mn^{2+} cations are adsorbed from the solution onto the surface layer of the carbon spheres through electrostatic interaction. (3) With the addition of APS and $AgNO_3$ solution, MnO_2 grows on the surface of the carbon spheres by a homogeneous catalytic route, whereas carbon spheres are oxidized, which results in the final MnO_2 hollow or porous, urchin-like spheres. We deduce that we can control the size of the inner pore through the size of the carbon spheres (Scheme 1). It is reasonable to deduce that various hollow structures of metal oxides with different morphologies could be produced by utilizing diverse reactive carbon templates.

Figure 6 shows the N_2 adsorption and desorption isotherm and the BJH (Barret–Joyner–Halenda) pore-size distribution curve (inset) of the γ-MnO_2 hollow urchin spheres. This kind of isotherm indicates that the γ-MnO_2 hollow urchins belong to the mesoporous family with the average pore-size distribution of 17 nm. The BET specific surface area of γ-MnO_2 calculated from N_2 adsorption at 77.4 K is 110 $m^2 g^{-1}$.

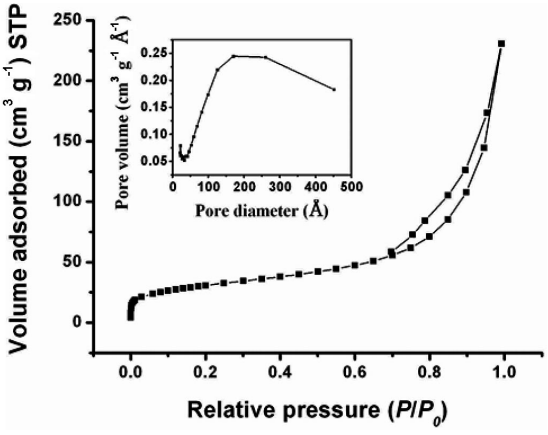

Figure 6. N_2 adsorption–desorption isotherm and BJH pore-size distribution plot (inset) of γ-MnO_2 hollow urchins.

The magnetic properties of the γ-MnO_2 hollow urchins were determined with a Quantum Design MPMS-5 SQUID magnetometer. Figure 7a shows the magnetization versus temperature (M–T) curve of the as-obtained γ-MnO_2 hollow urchins at an applied field strength of 1000 Oe. The M–T curve in the low-temperature region shows a strong concave nature without showing any distinct magnetic phase transition. The inverse of the magnetization of the γ-MnO_2 hollow urchins is shown in the inset of Figure 7a. A typical Curie–Weiss behavior is observed above 100 K. Least-squares fit of the linear portion of the curve above 100 K gives a negative Weiss temperature (θ) for γ-MnO_2 hollow urchins. The value of θ is –178.6 K. Considering the large increase in the magnetization below 50 K and the large negative value of the Weiss temperature, it can be considered that the γ-MnO_2 hollow urchins are ferrimagnetic. To further substantiate this deduction, the magnetization as a function of field H was measured at 2 K. A nearly linear M–H curve (Figure 7b) reveals that the γ-MnO_2 hollow urchins are paramagnetic, but they are not truly paramagnetic at this temperature. A small deviation from the expected paramagnetic behavior is observed for higher fields in the 2 K region. This is possible if the sample is a mixture of major paramagnetic and minor ferrimagnetic phases.

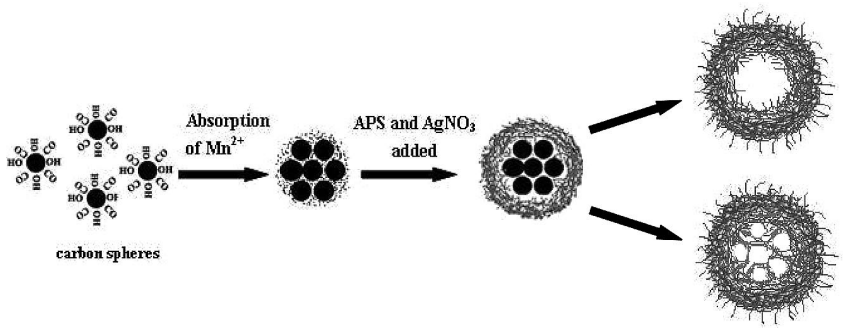

Scheme 1. Schematic illustration of the mechanism of formation of the hollow or porous, urchin-like γ-MnO_2 spheres synthesized by the carbon spheres reactive template method.

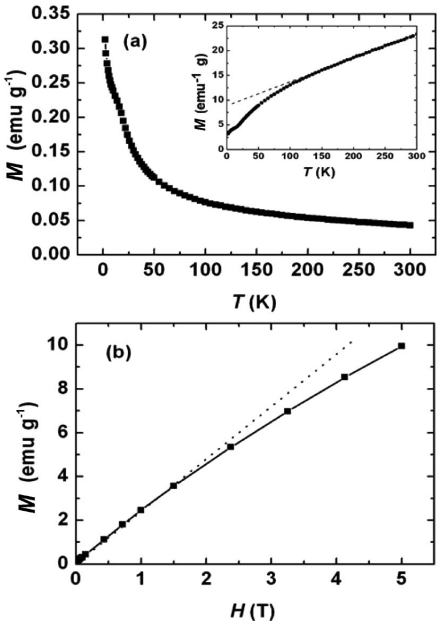

Figure 7. (a) Magnetization vs. temperature curve of the as-obtained γ-MnO_2 hollow urchins at an applied field of 1000 Oe, (b) magnetization vs. applied magnetic field strength of the as-obtained γ-MnO_2 hollow urchins at 2 K.

Conclusions

We developed a novel and facile carbon-based reactive template method to fabricate manganese oxide hollow spheres with an urchin-like morphology on a large scale. In comparison to reported conventional template methods, the carbon spheres template method does not require additional dissolution or a calcination process to remove the template after reaction, because it can be oxidized and removed in APS and $AgNO_3$ solutions. The formation mechanism of the γ-MnO_2 hollow urchins was investigated. We suggest that this method will open a way to explore the preparation of metal oxides with various morphologies through diverse morphologies of the reactive carbon template.

Experimental Section

Materials: All chemicals were of analytical grade and used as purchased without further purification. Glucose, APS, $MnSO_4 \cdot H_2O$, and $AgNO_3$ were all supplied by the Beijing Chemical Factory.

Preparation of Template Carbon Spheres: The colloidal carbon spheres (CCSs) were prepared according to the literature.[29] Glucose (4 g) was dissolved in water (40 mL) to form a transparent solution, which was placed in a 40-mL Teflon-sealed autoclave and heated at 160 °C for 4–20 h. A black or dark-purple precipitate was washed with water or ethanol, respectively. The final carbon spheres were obtained after oven drying at 80 °C for more than 4 h.

Preparation of Manganese Oxide Hollow Urchins: A typical synthesis of γ-MnO_2 hollow urchins was performed as follows: The carbon spheres were dispersed into a $MnSO_4$ solution (0.04 M, 50 mL) and ultrasonicated for 40–80 min to allow uniform adsorption of the manganese ions on the surface of the carbon spheres. Then, solutions of APS (10 mL, 6 mmol) and $AgNO_3$ (0.0177 mmol) were added into the above mixture, and the solution was magnetically stirred for 2 d at room temperature. The black solid precipitate was filtered off, washed with distilled water and absolute ethanol several times, and then dried under vacuum at 60 °C for 3 h.

Characterization: FTIR spectra were obtained with an Alpha-Centauri 650 spectrometer. XRD patterns of the as-prepared samples were recorded with a Japan Rigaku Dmax 2000 X-ray diffractometer with Cu-K_α radiation. A scanning rate of 4° min^{-1} was applied to record the pattern in the 2θ range of 3–90°. SEM equipped with energy-dispersive spectroscopy was performed with a XL-30 ESEM FEG scanning electron microscope operated at 20 kV with gold sputtered on samples. A Hitachi H-800 TEM operating at 20 kV accelerating voltage was used for TEM analysis. N_2 adsorption–desorption isotherms were performed with a Micromeritics NOVA-1000 apparatus with nitrogen as the analysis gas. The pore diameter and the pore-size distribution at the shell were determined by the BJH method. Magnetic measurements were performed with a Quantum Design MPMS-5 SQUID magnetometer.

Acknowledgments

This work was supported by the Program for Changjiang Scholars and Innovative Research Team in University and the Science Foundation of Jilin Province (20070505)

[1] H. L. Xu, W. Z. Wang, *Angew. Chem.* **2007**, *119*, 1511–1514; *Angew. Chem. Int. Ed.* **2007**, *46*, 1489–1492.
[2] X. X. Li, Y. J. Xiong, Z. Q. Li, Y. Xie, *Inorg. Chem.* **2006**, *45*, 3439–3445.
[3] D. B. Wang, *J. Phys. Chem. B* **2005**, *109*, 1125–1129.
[4] X. M. Sun, Y. D. Li, *Angew. Chem.* **2004**, *116*, 3915–3919; *Angew. Chem. Int. Ed.* **2004**, *43*, 3827–3831.
[5] L. L. Li, Y. Chu, Y. Liu, L. H. Dong, *J. Phys. Chem. C* **2007**, *111*, 2123–2127.
[6] X. L. Li, T. J. Lou, X. M. Sun, Y. D. Li, *Inorg. Chem.* **2004**, *43*, 5442–5449.
[7] R. A. Caruso, A. Susha, F. Caruso, *Chem. Mater.* **2001**, *13*, 400–409.
[8] S. Y. Chang, L. S. Liu, A. Asher, *J. Am. Chem. Soc.* **1994**, *116*, 6745–6747.
[9] X. M. Sun, J. F. Liu, Y. D. Li, *Chem. Eur. J.* **2006**, *12*, 2039–2047.
[10] D. Walsh, S. Mann, *Nature* **1995**, *377*, 320–323.
[11] H. T. Schmidt, A. E. Ostafin, *Adv. Mater.* **2002**, *14*, 532–535.
[12] T. Liu, Y. Xie, B. Chu, *Langmuir* **2000**, *16*, 9015–9022.
[13] Z. M. Zhang, J. Sui, L. J. Zhang, M. X. Wan, Y. Wei, L. M. Yu, *Adv. Mater.* **2005**, *17*, 2854 –2857.
[14] L. J. Pan, L. Pu, Y. Shi, S. Y. Song, Z. Xu, R. Zhang, Y. D. Zheng, *Adv. Mater.* **2007**, *19*, 461–464.
[15] a) A. Dong, N. Ren, Y. Tang, Y. Wang, Y. Zhang, W. Hua, Z. Gao, *J. Am. Chem. Soc.* **2003**, *125*, 4976–4977; b) Z. Yang, Y. Xia, R. Mokaya, *Adv. Mater.* **2004**, *16*, 727–732.
[16] R. Yuan, X. Fu, X. Wang, P. Liu, L. Wu, Y. Xu, X. Wang, Z. Wang, *Chem. Mater.* **2006**, *18*, 4700–4705.
[17] Y. C. Son, V. D. Makwana, A. R. Howell, S. L. Suib, *Angew. Chem. Int. Ed.* **2001**, *40*, 4280–4283.
[18] O. Giraldo, S. L. Brock, W. S. Willis, M. Marquez, S. L. Suib, S. Ching, *J. Am. Chem. Soc.* **2000**, *122*, 9330–9331.
[19] W. N. Li, J. K. Yuan, X. F. Shen, S. G. Mower, L. P. Xu, S. Sithambaram, M. Aindow, S. L. Suib, *Adv. Funct. Mater.* **2006**, *16*, 1247–1253.
[20] F. Y. Cheng, J. Z. Zhao, W. N. Song, C. S. Li, H. Ma, J. Chen, P. W. Shen, *Inorg. Chem.* **2006**, *45*, 2038–2044.

[21] J. Y. Luo, J. J. Zhang, Y. Y. Xia, *Chem. Mater.* **2006**, *18*, 5618–5623.
[22] Y. Xiong, Y. Xie, Z. Li, C. Wu, *Chem. Eur. J.* **2003**, *9*, 1645–1651.
[23] X. Wang, Y. D. Li, *J. Am. Chem. Soc.* **2002**, *124*, 2880–2881.
[24] S. Zhu, H. Zhou, M. Hibino, I. Honma, M. Ichihara, *Adv. Funct. Mater.* **2005**, *15*, 381–386.
[25] J. Fan, T. Wang, C. Yu, B. Tu, Z. Jiang, D. Zhao, *Adv. Mater.* **2004**, *16*, 1432–1436.
[26] W. C. Choi, S. I. Woo, M. K. Jeon, J. M. Sohn, M. R. Kim, H. J. Jeon, *Adv. Mater.* **2005**, *17*, 446–451.
[27] J. K. Yuan, K. Laubernds, Q. H. Zhang, S. L. Suib, *J. Am. Chem. Soc.* **2003**, *125*, 4966–4967.
[28] Z. Q. Li, Y. Ding, Y. J. Xiong, Y. Xie, *Cryst. Growth Des.* **2005**, *5*, 1953–1958.
[29] X. M. Sun, Y. D. Li, *Angew. Chem. Int. Ed.* **2004**, *43*, 597–601.
[30] C. Julien, M. Massot, S. Rangan, M. Lemal, D. Guyomard, *J. Raman Spectrosc.* **2002**, *33*, 223–228.
[31] C. Z. Wu, Y. Xie, D. Wang, J. Yang, T. W. Li, *J. Phys. Chem. B* **2003**, *107*, 13583–13587.
[32] Z. Q. Li, Y. Ding, Y. J. Xiong, Y. Xie, *Cryst. Growth Des.* **2005**, *5*, 1953–1958.
[33] D. A. House, *Chem. Rev.* **1962**, *62*, 185–203.
[34] Y. K. Gupta, S. Ghosh, *J. Lnorg. Nucl. Chem.* **1959**, *9*, 178–183.
[35] A. A. Noyesa, A. Kossiakoff, *J. Am. Chem. Soc.* **1935**, *57*, 1238–1242.
[36] Q. F. Ye, C. Y. Wang, D. H. Wang, G. Sun, X. H. Xu, J. Zhejiang, *Univ. Science B* **2006**, *7*, 404–410.
[37] C. Brandt, R. V. Eldik, *Chem. Rev.* **1995**, *95*, 119–190.
[38] H. Y. Wang, J. H. Qu, *Water Res.* **2003**, *37*, 3767–3775.

Received: March 6, 2008
Published Online: July 9, 2008

